Observation of Top Quark Production in $\bar{p}p$ Collisions with the Collider Detector at Fermilab

F. Abe,[14] H. Akimoto,[32] A. Akopian,[27] M. G. Albrow,[7] S. R. Amendolia,[24] D. Amidei,[17] J. Antos,[29] C. Anway-Wiese,[4] S. Aota,[32] G. Apollinari,[27] T. Asakawa,[32] W. Ashmanskas,[15] M. Atac,[7] P. Auchincloss,[26] F. Azfar,[22] P. Azzi-Bacchetta,[21] N. Bacchetta,[21] W. Badgett,[17] S. Bagdasarov,[27] M. W. Bailey,[19] J. Bao,[35] P. de Barbaro,[26] A. Barbaro-Galtieri,[15] V. E. Barnes,[25] B. A. Barnett,[13] P. Bartalini,[24] G. Bauer,[16] T. Baumann,[9] F. Bedeschi,[24] S. Behrends,[3] S. Belforte,[24] G. Bellettini,[24] J. Bellinger,[34] D. Benjamin,[31] J. Benlloch,[16] J. Bensinger,[3] D. Benton,[22] A. Beretvas,[7] J. P. Berge,[7] S. Bertolucci,[8] A. Bhatti,[27] K. Biery,[12] M. Binkley,[7] D. Bisello,[21] R. E. Blair,[1] C. Blocker,[3] A. Bodek,[26] W. Bokhari,[16] V. Bolognesi,[24] D. Bortoletto,[25] J. Boudreau,[23] G. Brandenburg,[9] L. Breccia,[2] C. Bromberg,[18] E. Buckley-Geer,[7] H. S. Budd,[26] K. Burkett,[17] G. Busetto,[21] A. Byon-Wagner,[7] K. L. Byrum,[1] J. Cammerata,[13] C. Campagnari,[7] M. Campbell,[17] A. Caner,[7] W. Carithers,[15] D. Carlsmith,[34] A. Castro,[21] G. Cauz,[24] Y. Cen,[26] F. Cervelli,[24] H. Y. Chao,[29] J. Chapman,[17] M.-T. Cheng,[29] G. Chiarelli,[24] T. Chikamatsu,[32] C. N. Chiou,[29] L. Christofek,[11] S. Cihangir,[7] A. G. Clark,[24] M. Cobal,[24] M. Contreras,[5] J. Conway,[28] J. Cooper,[7] M. Cordelli,[8] C. Couyoumtzelis,[24] D. Crane,[1] D. Cronin-Hennessy,[6] R. Culbertson,[5] J. D. Cunningham,[3] T. Daniels,[16] F. DeJongh,[7] S. Delchamps,[7] S. Dell'Agnello,[24] M. Dell'Orso,[24] L. Demortier,[27] B. Denby,[24] M. Deninno,[2] P. F. Derwent,[17] T. Devlin,[28] M. Dickson,[26] J. R. Dittmann,[6] S. Donati,[24] R. B. Drucker,[15] A. Dunn,[17] N. Eddy,[17] K. Einsweiler,[15] J. E. Elias,[7] R. Ely,[15] E. Engels, Jr.,[23] D. Errede,[11] S. Errede,[11] Q. Fan,[26] I. Fiori,[2] B. Flaugher,[7] G. W. Foster,[7] M. Franklin,[9] M. Frautschi,[19] J. Freeman,[7] J. Friedman,[16] H. Frisch,[5] T. A. Fuess,[1] Y. Fukui,[14] S. Funaki,[32] G. Gagliardi,[23] S. Galeotti,[24] M. Gallinaro,[21] M. Garcia-Sciveres,[15] A. F. Garfinkel,[25] C. Gay,[9] S. Geer,[7] D. W. Gerdes,[17] P. Giannetti,[24] N. Giokaris,[27] P. Giromini,[8] L. Gladney,[22] D. Glenzinski,[13] M. Gold,[19] J. Gonzalez,[22] A. Gordon,[9] A. T. Goshaw,[6] K. Goulianos,[27] H. Grassmann,[7,*] L. Groer,[28] C. Grosso-Pilcher,[5] G. Guillian,[17] R. S. Guo,[29] C. Haber,[15] S. R. Hahn,[7] R. Hamilton,[9] R. Handler,[34] R. M. Hans,[35] K. Hara,[32] B. Harral,[22] R. M. Harris,[7] S. A. Hauger,[6] J. Hauser,[4] C. Hawk,[28] E. Hayashi,[32] J. Heinrich,[22] M. Hohlmann,[1,5] C. Holck,[22] R. Hollebeek,[22] L. Holloway,[11] A. Hölscher,[12] S. Hong,[17] G. Houk,[22] P. Hu,[23] B. T. Huffman,[23] R. Hughes,[26] J. Huston,[18] J. Huth,[9] J. Hylen,[7] H. Ikeda,[32] M. Incagli,[24] J. Incandela,[7] J. Iwai,[32] Y. Iwata,[10] H. Jensen,[7] U. Joshi,[7] R. W. Kadel,[15] E. Kajfasz,[7,*] T. Kamon,[30] T. Kaneko,[32] K. Karr,[33] H. Kasha,[35] Y. Kato,[20] L. Keeble,[8] K. Kelley,[16] R. D. Kennedy,[28] R. Kephart,[7] P. Kesten,[15] D. Kestenbaum,[9] R. M. Keup,[11] H. Keutelian,[7] F. Keyvan,[4] B. J. Kim,[26] D. H. Kim,[7,*] H. S. Kim,[12] S. B. Kim,[17] S. H. Kim,[32] Y. K. Kim,[15] L. Kirsch,[3] P. Koehn,[26] K. Kondo,[32] J. Konigsberg,[9] S. Kopp,[5] K. Kordas,[12] W. Koska,[7] E. Kovacs,[7,*] W. Kowald,[6] M. Krasberg,[17] J. Kroll,[7] M. Kruse,[25] T. Kuwabara,[32] S. E. Kuhlmann,[1] E. Kuns,[28] A. T. Laasanen,[25] N. Labanca,[24] S. Lammel,[7] J. I. Lamoureux,[3] T. LeCompte,[11] S. Leone,[24] J. D. Lewis,[7] P. Limon,[7] M. Lindgren,[4] T. M. Liss,[11] N. Lockyer,[22] O. Long,[22] C. Loomis,[28] M. Loreti,[21] J. Lu,[30] D. Lucchesi,[24] P. Lukens,[7] S. Lusin,[34] J. Lys,[15] K. Maeshima,[7] A. Maghakian,[27] P. Maksimovic,[16] M. Mangano,[24] J. Mansour,[18] M. Mariotti,[21] J. P. Marriner,[7] A. Martin,[11] J. A. J. Matthews,[19] R. Mattingly,[16] P. McIntyre,[30] P. Melese,[27] A. Menzione,[24] E. Meschi,[24] S. Metzler,[22] C. Miao,[17] G. Michail,[9] S. Mikamo,[14] R. Miller,[18] H. Minato,[32] S. Miscetti,[8] M. Mishina,[14] H. Mitsushio,[32] T. Miyamoto,[32] S. Miyashita,[32] Y. Morita,[14] J. Mueller,[23] A. Mukherjee,[7] T. Muller,[4] P. Murat,[24] H. Nakada,[32] I. Nakano,[32] C. Nelson,[7] D. Neuberger,[4] C. Newman-Holmes,[7] M. Ninomiya,[32] L. Nodulman,[1] S. Ogawa,[32] S. H. Oh,[6] K. E. Ohl,[35] T. Ohmoto,[10] T. Ohsugi,[10] R. Oishi,[32] M. Okabe,[32] T. Okusawa,[20] R. Oliver,[22] J. Olsen,[34] C. Pagliarone,[2] R. Paoletti,[24] V. Papadimitriou,[31] S. P. Pappas,[35] S. Park,[7] J. Patrick,[7] G. Pauletta,[24] M. Paulini,[15] L. Pescara,[21] M. D. Peters,[15] T. J. Phillips,[6] G. Piacentino,[2] M. Pillai,[26] K. T. Pitts,[7] R. Plunkett,[7] L. Pondrom,[34] J. Proudfoot,[1] F. Ptohos,[9] G. Punzi,[24] K. Ragan,[12] A. Ribon,[21] F. Rimondi,[2] L. Ristori,[24] W. J. Robertson,[6] T. Rodrigo,[7,*] J. Romano,[5] L. Rosenson,[16] R. Roser,[11] W. K. Sakumoto,[26] D. Saltzberg,[5] A. Sansoni,[8] L. Santi,[24] H. Sato,[32] V. Scarpine,[30] P. Schlabach,[9] E. E. Schmidt,[7] M. P. Schmidt,[35] G. F. Sciacca,[24] A. Scribano,[24] S. Segler,[7] S. Seidel,[19] Y. Seiya,[32] G. Sganos,[12] A. Sgolacchia,[2] M. D. Shapiro,[15] N. M. Shaw,[25] Q. Shen,[25] P. F. Shepard,[23] M. Shimojima,[32] M. Shochet,[5] J. Siegrist,[15] A. Sill,[31] P. Sinervo,[12] P. Singh,[23] J. Skarha,[13] K. Sliwa,[33] D. A. Smith,[24] F. D. Snider,[13] T. Song,[17] J. Spalding,[7] P. Sphicas,[16] L. Spiegel,[7] A. Spies,[13] L. Stanco,[21] J. Steele,[34] A. Stefanini,[24] K. Strahl,[12] J. Strait,[7] D. Stuart,[7] G. Sullivan,[5] A. Soumarokov,[29] K. Sumorok,[16] J. Suzuki,[32] T. Takada,[32] T. Takahashi,[20] T. Takano,[32] K. Takikawa,[32] N. Tamura,[10] F. Tartarelli,[24] W. Taylor,[12] P. K. Teng,[29] Y. Teramoto,[20] S. Tether,[16] D. Theriot,[7] T. L. Thomas,[19] R. Thun,[17] M. Timko,[33] P. Tipton,[26] A. Titov,[27] S. Tkaczyk,[7] D. Toback,[5] K. Tollefson,[26] A. Tollestrup,[7] J. Tonnison,[25] J. F. de Troconiz,[9] S. Truitt,[17] J. Tseng,[13] N. Turini,[24] T. Uchida,[32] N. Uemura,[32] F. Ukegawa,[22] G. Unal,[22] S. C. van den Brink,[23] S. Vejcik III,[17] G. Velev,[24] R. Vidal,[7] M. Vondracek,[11] D. Vucinic,[16] R. G. Wagner,[1] R. L. Wagner,[7] J. Wahl,[5] R. C. Walker,[26] C. Wang,[6] C. H. Wang,[29] G. Wang,[24] J. Wang,[5] M. J. Wang,[29] Q. F. Wang,[27] A. Warburton,[12] G. Watts,[26] T. Watts,[28] R. Webb,[30] C. Wei,[6] C. Wendt,[34] H. Wenzel,[15] W. C. Wester III,[7] A. B. Wicklund,[1] E. Wicklund,[7] R. Wilkinson,[22] H. H. Williams,[22] P. Wilson,[5] B. L. Winer,[26] D. Wolinski,[17] J. Wolinski,[30] X. Wu,[24] J. Wyss,[21] A. Yagil,[7] W. Yao,[15]

K. Yasuoka,[32] Y. Ye,[12] G. P. Yeh,[7] P. Yeh,[29] M. Yin,[6] J. Yoh,[7] C. Yosef,[18] T. Yoshida,[20] D. Yovanovitch,[7] I. Yu,[35] J. C. Yun,[7] A. Zanetti,[24] F. Zetti,[24] L. Zhang,[34] W. Zhang,[22] and S. Zucchelli[2]

(CDF Collaboration)

[1]Argonne National Laboratory, Argonne, Illinois 60439
[2]Istituto Nazionale di Fisica Nucleare, University of Bologna, I-40126 Bologna, Italy
[3]Brandeis University, Waltham, Massachusetts 02254
[4]University of California at Los Angeles, Los Angeles, California 90024
[5]University of Chicago, Chicago, Illinois 60637
[6]Duke University, Durham, North Carolina 27708
[7]Fermi National Accelerator Laboratory, Batavia, Illinois 60510
[8]Laboratori Nazionali di Frascati, Istituto Nazionale di Fisica Nucleare, I-00044 Frascati, Italy
[9]Harvard University, Cambridge, Massachusetts 02138
[10]Hiroshima University, Higashi-Hiroshima 724, Japan
[11]University of Illinois, Urbana, Illinois 61801
[12]Institute of Particle Physics, McGill University, Montreal, Canada H3A 2T8
and University of Toronto, Toronto, Canada M5S 1A7
[13]The Johns Hopkins University, Baltimore, Maryland 21218
[14]National Laboratory for High Energy Physics (KEK), Tsukuba, Ibaraki 305, Japan
[15]Lawrence Berkeley Laboratory, Berkeley, California 94720
[16]Massachusetts Institute of Technology, Cambridge, Massachusetts 02139
[17]University of Michigan, Ann Arbor, Michigan 48109
[18]Michigan State University, East Lansing, Michigan 48824
[19]University of New Mexico, Albuquerque, New Mexico 87131
[20]Osaka City University, Osaka 588, Japan
[21]Università di Padova, Instituto Nazionale di Fisica Nucleare, Sezione di Padova, I-35131 Padova, Italy
[22]University of Pennsylvania, Philadelphia, Pennsylvania 19104
[23]University of Pittsburgh, Pittsburgh, Pennsylvania 15260
[24]Istituto Nazionale di Fisica Nucleare, University and Scuola Normale Superiore of Pisa, I-56100 Pisa, Italy
[25]Purdue University, West Lafayette, Indiana 47907
[26]University of Rochester, Rochester, New York 14627
[27]Rockefeller University, New York, New York 10021
[28]Rutgers University, Piscataway, New Jersey 08854
[29]Academia Sinica, Taipei, Taiwan 11529, Republic of China
[30]Texas A&M University, College Station, Texas 77843
[31]Texas Tech University, Lubbock, Texas 79409
[32]University of Tsukuba, Tsukuba, Ibaraki 305, Japan
[33]Tufts University, Medford, Massachusetts 02155
[34]University of Wisconsin, Madison, Wisconsin 53706
[35]Yale University, New Haven, Connecticut 06511
(Received 24 February 1995)

We establish the existence of the top quark using a 67 pb^{-1} data sample of $\bar{p}p$ collisions at $\sqrt{s} = 1.8$ TeV collected with the Collider Detector at Fermilab (CDF). Employing techniques similar to those we previously published, we observe a signal consistent with $t\bar{t}$ decay to $WWb\bar{b}$, but inconsistent with the background prediction by 4.8σ. Additional evidence for the top quark is provided by a peak in the reconstructed mass distribution. We measure the top quark mass to be $176 \pm 8(\text{stat}) \pm 10(\text{syst})$ GeV/c^2, and the $t\bar{t}$ production cross section to be $6.8^{+3.6}_{-2.4}$ pb.

Recently the Collider Detector at Fermilab (CDF) Collaboration presented the first direct evidence for the top quark [1], the weak isodoublet partner of the b quark required in the standard model. We searched for $t\bar{t}$ pair production with the subsequent decay $t\bar{t} \rightarrow Wb W\bar{b}$. The observed topology in such events is determined by the decay mode of the two W bosons. Dilepton events ($e\mu$, ee, and $\mu\mu$) are produced primarily when both W bosons decay into $e\nu$ or $\mu\nu$. Events in the lepton + jets channel (e, μ + jets) occur when one

W boson decays into leptons and the other decays into quarks. To suppress background in the lepton + jets mode, we identify b quarks by reconstructing secondary vertices from b decay (SVX tag) and by finding additional leptons from b semileptonic decay (SLT tag). In Ref. [1] we found a 2.8σ excess of signal over the expectation from background. The interpretation of the excess as top quark production was supported by a peak in the mass distribution for fully reconstructed events. Additional evidence was found in the jet energy distributions

in lepton + jets events [2]. An upper limit on the $t\bar{t}$ production cross section has been published by the D0 Collaboration [3].

We report here on a data sample containing 19 pb^{-1} used in Ref. [1] and 48 pb^{-1} from the current Fermilab Collider run, which began early in 1994 and is expected to continue until the end of 1995.

The CDF consists of a magnetic spectrometer surrounded by calorimeters and muon chambers [4]. A new low-noise, radiation-hard, four-layer silicon vertex detector, located immediately outside the beampipe, provides precise track reconstruction in the plane transverse to the beam and is used to identify secondary vertices from b and c quark decays [5]. The momenta of charged particles are measured in the central tracking chamber (CTC), which is in a 1.4 T superconducting solenoidal magnet. Outside the CTC, electromagnetic and hadronic calorimeters cover the pseudorapidity region $|\eta| < 4.2$ [6] and are used to identify jets and electron candidates. The calorimeters are also used to measure the missing transverse energy $\not{E}_T$, which can indicate the presence of undetected energetic neutrinos. Outside the calorimeters, drift chambers in the region $|\eta| < 1.0$ provide muon identification. A three-level trigger selects the inclusive electron and muon events used in this analysis. To improve the $t\bar{t}$ detection efficiency, triggers based on $\not{E}_T$ are added to the lepton triggers used in Ref. [1].

The data samples for both the dilepton and lepton + jets analyses are subsets of a sample of high-P_T inclusive lepton events that contain an isolated electron with $E_T > 20$ GeV or an isolated muon with $P_T > 20$ GeV/c in the central region ($|\eta| < 1.0$). Events which contain a second lepton candidate are removed as possible Z bosons if an ee or $\mu\mu$ invariant mass is between 75 and 105 GeV/c^2. For the lepton + jets analysis, an inclusive W boson sample is made by requiring $\not{E}_T > 20$ GeV. Table I classifies the W events by the number of jets with observed $E_T > 15$ GeV and $|\eta| < 2.0$. The dilepton sample consists of inclusive lepton events that also have a second lepton with $P_T > 20$ GeV/c, satisfying looser lepton identification requirements. The two leptons must have opposite electric charge.

The primary method for finding top quarks in the lepton + jets channel is to search for secondary vertices

TABLE I. Number of lepton + jet events in the 67 pb^{-1} data sample along with the numbers of SVX tags observed and the estimated background. Based on the excess number of tags in events with ≥ 3 jets, we expect an additional 0.5 and 5 tags from $t\bar{t}$ decay in the 1- and 2-jet bins, respectively.

N_{jet}	Observed events	Observed SVX tags	Background tags expected
1	6578	40	50 ± 12
2	1026	34	21.2 ± 6.5
3	164	17	5.2 ± 1.7
≥4	39	10	1.5 ± 0.4

from b quark decay (SVX tagging). The vertex-finding efficiency is significantly larger now than previously due to an improved vertex-finding algorithm and the performance of the new vertex detector. The previous vertex-finding algorithm searched for a secondary vertex with two or more tracks. The new algorithm first searches for vertices with three or more tracks with looser track requirements, and if that fails, searches for two-track vertices using more stringent track and vertex quality criteria. The efficiency for tagging a b quark is measured in inclusive electron and muon samples which are enriched in b decays. The ratio of the measured efficiency to the prediction of a detailed Monte Carlo simulation is 0.96 ± 0.07, with good agreement ($\pm 2\%$) between the electron and muon samples. The efficiency for tagging at least one b quark in a $t\bar{t}$ event with ≥ 3 jets is determined from Monte Carlo simulation to be $(42 \pm 5)\%$ in the current run, compared to the $(22 \pm 6)\%$ reported in the previous publication [7]. In this Letter we apply the new vertex-finding algorithm to the data from the previous and the current runs.

In Ref. [1], we presented two methods for estimating the background to the top quark signal. In method 1, the observed tag rate in inclusive jet samples is used to calculate the background from mistags and QCD-produced heavy quark pairs ($b\bar{b}$ and $c\bar{c}$) recoiling against a W boson. This is an overestimate of the background because there are sources of heavy quarks in an inclusive jet sample that are not present in W + jet events. In method 2, the mistag rate is again measured with inclusive jets, while the fraction of W + jet events that are $Wb\bar{b}$ and $Wc\bar{c}$ is estimated from a Monte Carlo sample, using measured tagging efficiencies. In the present analysis, we use method 2 as the best estimate of the SVX-tag background. The improved performance of the new vertex detector, our ability to simulate its behavior accurately, and the agreement between the prediction and data in the W + 1-jet and W + 2-jet samples make this the natural choice. The calculated background, including the small contributions from non-W background, Wc production, and vector boson pair production, is given in Table I.

The numbers of SVX tags in the 1-jet and 2-jet samples are consistent with the expected background plus a small $t\bar{t}$ contribution (Table I and Fig. 1). However, for the $W + \geq 3$-jet signal region, 27 tags are observed compared to a predicted background of 6.7 ± 2.1 tags [8]. The probability of the background fluctuating to ≥ 27 is calculated to be 2×10^{-5} (see Table II) using the procedure outlined in Ref. [1] (see [9]). The 27 tagged jets are in 21 events; the six events with two tagged jets can be compared with four expected for the top + background hypothesis and ≤ 1 for background alone. Figure 1 also shows the decay lifetime distribution for the SVX tags in $W + \geq 3$-jet events. It is consistent with the distribution predicted for b decay from the $t\bar{t}$ Monte Carlo simulation. From the number of SVX-tagged events, the estimated background, the calculated
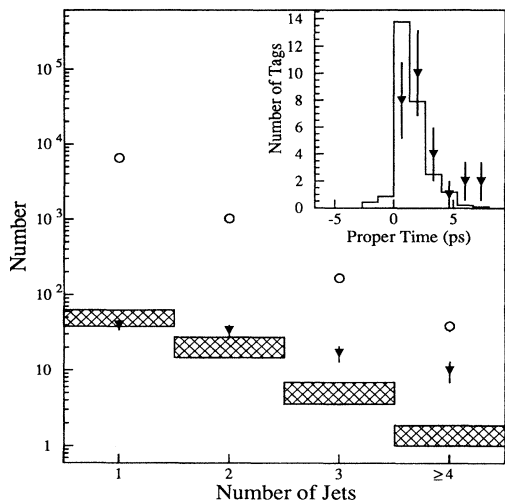
FIG. 1. Number of events before SVX tagging (circles), number of tags observed (triangles), and expected number of background tags (hatched) versus jet multiplicity. Based on the excess number of tags in events with ≥3 jets, we expect an additional 0.5 and 5 tags from $t\bar{t}$ decay in the 1- and 2-jet bins, respectively. The inset shows the secondary vertex proper time distribution for the 27 tagged jets in the $W+$ ≥3-jet data (triangles) compared to the expectation for b quark jets from $t\bar{t}$ decay.

$t\bar{t}$ acceptance, and the integrated luminosity of the data sample, we calculate the $t\bar{t}$ production cross section to be $6.8^{+3.6}_{-2.4}$ pb, where the uncertainty includes both statistical and systematic effects. This differs from the cross section given in Ref. [1] by 6.9 ± 5.9 pb.

The second technique for tagging b quarks (SLT tagging) is to search for an additional lepton from semileptonic b decay. Electrons and muons are found by matching CTC tracks with electromagnetic energy clusters or tracks in the muon chambers. To maintain acceptance for leptons coming directly from b decay and from the daughter c quark, the P_T threshold is kept low (2 GeV/c). The only significant change to the selection algorithm compared to Ref. [1] is that the fiducial region for SLT muons has been increased from $|\eta| < 0.6$ to $|\eta| < 1.0$, resulting in an increase of the SLT total acceptance and background by a factor of 1.2.

The major backgrounds in the SLT analysis are hadrons that are misidentified as leptons, and electrons from unidentified photon conversions. These rates and the smaller $Wb\bar{b}$ and $Wc\bar{c}$ backgrounds are determined di-

TABLE II. The number of tags or events observed in the three channels along with the expected background and the probability that the background would fluctuate to the observed number or more.

Channel	SVX	SLT	Dilepton
Observed	27 tags	23 tags	6 events
Expected background	6.7 ± 2.1	15.4 ± 2.0	1.3 ± 0.3
Background probability	2×10^{-5}	6×10^{-2}	3×10^{-3}

rectly from inclusive jet data. The remaining backgrounds are much smaller and are calculated using the techniques discussed in Ref. [1]. The efficiency of the algorithm is measured with photon conversion and $J/\psi \rightarrow \mu\mu$ data. The probability of finding an additional e or μ in a $t\bar{t}$ event with ≥3 jets is (20 ± 2)%. Table II shows the background and number of observed tags for the signal region ($W+$ ≥3 jets). There are 23 tags in 22 events, with 15.4 ± 2.0 tags expected from background. Six events contain both an SVX and SLT tag, compared to the expected four for top + background and one for background alone.

The dilepton analysis is very similar to that previously reported [1], with slight modifications to the lepton identification requirements to make them the same as those used in the single lepton analysis. The dilepton data sample, described above, is reduced by additional requirements on $\not{E}_T$ and the number of jets. In order to suppress background from Drell-Yan lepton pairs, which have little or no true $\not{E}_T$, the $\not{E}_T$ is corrected to account for jet energy mismeasurement [1]. The magnitude of the corrected $\not{E}_T$ is required to be at least 25 GeV and, if $\not{E}_T$ is less than 50 GeV, the azimuthal angle between the $\not{E}_T$ vector and the nearest lepton or jet must be greater than $20°$. Finally, all events are required to have at least two jets with observed $E_T > 10$ GeV and $|\eta| < 2.0$.

The major backgrounds are Drell-Yan lepton pairs, $Z \rightarrow \tau\tau$, hadrons misidentified as leptons, WW, and $b\bar{b}$ production. We calculate the first three from data and the last two with Monte Carlo simulation [1]. As is shown in Table II, the total background expected is 1.3 ± 0.3 events. We observe a total of seven events, 5 $e\mu$ and 2 $\mu\mu$. The relative numbers are consistent with our dilepton acceptance, 60% of which is in the $e\mu$ channel. Although we estimated the expected background from radiative Z decay to be small (0.04 event), one of the $\mu\mu$ events contains an energetic photon with a $\mu\mu\gamma$ invariant mass of 86 GeV/c^2. To be conservative, we removed that event from the final sample, which thus contains six events. Three of these events contain a total of five b tags, compared with an expected 0.5 if the events are background. We would expect 3.6 tags if the events are from $t\bar{t}$ decay. When the requirement that the leptons have opposite charge is relaxed, we find one same-sign dilepton event ($e\mu$) that passes all the other event selection criteria. The expected number of same-sign events is 0.5, of which 0.3 is due to background and 0.2 to $t\bar{t}$ decay.

In summary, we find 37 b-tagged $W+$ ≥3-jet events [10] that contain 27 SVX tags compared to 6.7 ± 2.1 expected from background and 23 SLT tags with an estimated background of 15.4 ± 2.0. There are six dilepton events compared to 1.3 ± 0.3 events expected from background. We have taken the product (P) of the three probabilities in Table II and calculated the likelihood that a fluctuation of the background alone would yield a value of P no larger than that which we observe. The result

2629

is 1×10^{-6}, which is equivalent to a 4.8σ deviation in a Gaussian distribution [11]. Based on the excess number of SVX-tagged events, we expect an excess of 7.8 SLT tags and 3.5 dilepton events from $t\bar{t}$ production, in good agreement with the observed numbers.

We performed a number of checks of this analysis. A good control sample for b tagging is Z + jet events, where no top contribution is expected. We observe 15, 3, and 2 tags (SVX and SLT) in the Z + 1-jet, 2-jet, and $\geq$3-jet samples, respectively, compared with the background predictions of 17.5, 4.2, and 1.5. The excess over background that was seen in Ref. [1] is no longer present. In addition, there is no discrepancy between the measured and predicted W + 4-jet background, in contrast to a small deficit described in Ref. [1] (see [12]).

Single-lepton events with four or more jets can be kinematically reconstructed to the $t\bar{t} \rightarrow Wb W\bar{b}$ hypothesis, yielding for each event an estimate of the top quark mass [1]. The lepton, neutrino ($\not{E}_T$), and the four highest-E_T jets are assumed to be the $t\bar{t}$ daughters [13]. There are multiple solutions, due to both the quadratic ambiguity in determining the longitudinal momentum of the neutrino and the assignment of jets to the parent W's and b's. For each event, the solution with the lowest fit χ^2 is chosen. Starting with the 203 events with $\geq$3 jets, we require each event to have a fourth jet with $E_T > 8$ GeV and $|\eta| < 2.4$. This yields a sample of 99 events, of which 88 pass a loose χ^2 requirement on the fit. The mass distribution for these events is shown in Fig. 2. The distribution is consistent with the predicted mix of approximately 30% $t\bar{t}$ signal and 70% W + jets background. The Monte Carlo background shape agrees well with that meaured in a limited-statistics sample of Z + 4-jet events

as well as in a QCD sample selected to approximate non-W background. After requiring an SVX or SLT b tag, 19 of the events remain, of which $6.9^{+2.5}_{-1.9}$ are expected to be background. For these events, only solutions in which the tagged jet is assigned to one of the b quarks are considered. Figure 3 shows the mass distribution for the tagged events. The mass distribution in the current run is very similar to that from the previous run. Furthermore, we employed several mass fitting techniques which give nearly identical results.

To find the most likely top mass, we fit the mass distribution to a sum of the expected distributions from the W + jets background and a top quark of mass M_{top} [1]. The $-\ln(\text{liklihood})$ distribution from the fit is shown in the Fig. 3 inset. The best fit mass is 176 GeV/c^2 with a ± 8 GeV/c^2 statistical uncertainty. We make a conservative extrapolation of the systematic uncertainty from our previous publication, giving $M_{\text{top}} = 176 \pm 8 \pm 10$ GeV/c^2. Further studies of systematic uncertainties are in progress.

The shape of the mass peak in Fig. 3 provides additional evidence for top quark production, since the number of observed b tags is independent of the observed mass distribution. After including systematic effects in the predicted background shape, we find a 2×10^{-2} probability that the observed mass distribution is consistent with the background (Kolmogorov-Smirnov test). This is a conservative measure because it does not explicitly take into account the observed narrow mass peak.

In conclusion, additional data confirm the top quark evidence presented in Ref. [1]. There is now a large

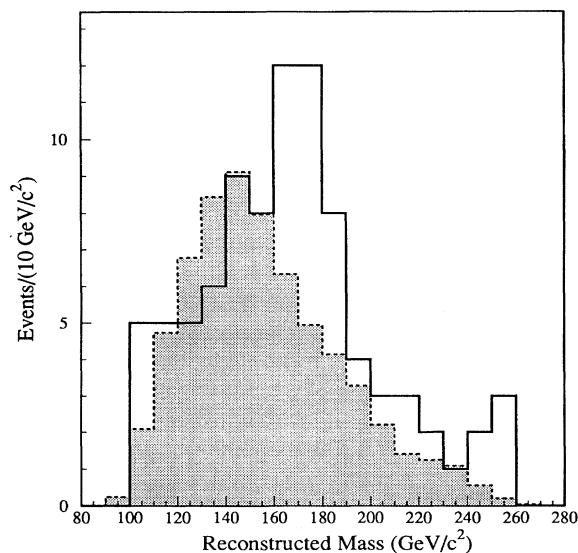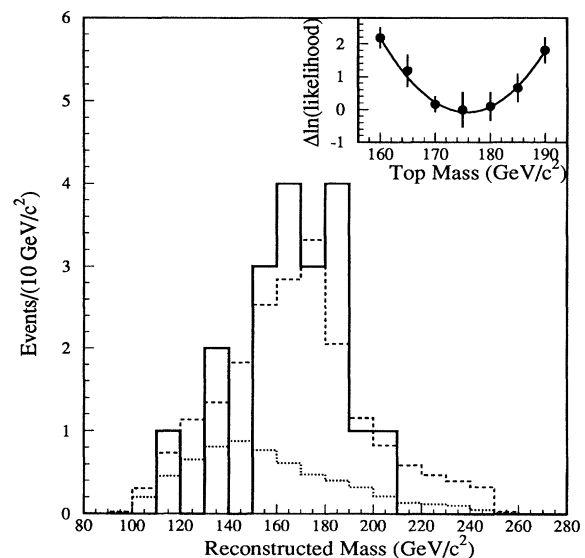FIG. 2. Reconstructed mass distribution for the W+ $\geq$4-jet sample prior to b tagging (solid). Also shown is the background distribution (shaded) with the normalization constrained to the calculated value.

FIG. 3. Reconstructed mass distribution for the b-tagged W+ $\geq$4-jet events (solid). Also shown are the background shape (dotted) and the sum of background plus $t\bar{t}$ Monte Carlo simulations for $M_{\text{top}} = 175$ GeV/c^2 (dashed), with the background constrained to the calculated value, $6.9^{+2.5}_{-1.9}$ events. The inset shows the likelihood fit used to determine the top mass.

excess in the signal that is inconsistent with the background prediction by 4.8σ, and a mass distribution with a 2×10^{-2} probability of being consistent with the background shape. When combined, the signal size and mass distribution have a 3.7×10^{-7} probability of satisfying the background hypothesis (5.0σ). In addition, a substantial fraction of the jets in the dilepton events are b tagged. This establishes the existence of the top quark. The preliminary mass and cross section measurements yield $M_{\text{top}} = 176 \pm 8 \pm 10 \text{ GeV}/c^2$ and $\sigma_{t\bar{t}} = 6.8^{+3.6}_{-2.4}$ pb.

*Visitor.

[1] F. Abe *et al.*, Phys. Rev. D **50**, 2966 (1994); Phys. Rev. Lett. **73**, 225 (1994).

[2] F. Abe *et al.*, Phys. Rev. D (to be published).

[3] S. Abachi *et al.*, Phys. Rev. Lett. **72**, 2138 (1994); following Letter, Phys. Rev. Lett. **74**, 2632 (1995).

[4] F. Abe *et al.*, Nucl. Instrum. Methods Phys. Res., Sect. A **271**, 387 (1988).

[5] P. Azzi *et al.*, Fermilab Report No. FERMILAB-CONF-94/205-E, 1994 (unpublished). Our previous silicon vertex detector is described in D. Amidei *et al.*, Nucl. Instrum. Methods Phys. Res., Sect. A **350**, 73 (1994).

[6] In the CDF coordinate system, θ is the polar angle with respect to the proton beam direction. The pseudorapidity η is defined as $-\ln \tan(\theta/2)$. The transverse momentum of a particle is $P_T = P \sin\theta$. If the magnitude of this vector is obtained using the calorimeter energy rather than the spectrometer momentum, it becomes the transverse energy E_T. The difference between the vector sum of all the transverse energies in an event and zero is the missing transverse energy $(\not{E}_T)$.

[7] A factor of 1.65 increase comes from the improvements noted. The remaining factor of 1.15 results from correcting an error in the b baryon lifetime used in the simulation of $t\bar{t}$ decay in Ref. [1].

[8] For comparison we note that if we had used both the tagging algorithm and background calculation (method 1) presented in Ref. [1], we would have 24 observed tags with a predicted background of 8.8 ± 0.6 tags.

[9] We get essentially the same probability if we use method 1 for the SVX-tag background because of its smaller systematic uncertainty.

[10] There are 21 events with SVX tags and 22 events with SLT tags. Six of these events have both SVX and SLT tags.

[11] This technique is chosen because we are combining channels with very different expected background rates. For comparison, if we apply the method used in Ref. [1] to the SVX and dilepton channels, the two low background modes, we obtain a probability of 1.5×10^{-6}.

[12] The improved agreement is due to the smaller $t\bar{t}$ production cross section obtained in this analysis as well as correcting an overestimate in Ref. [1] in the Monte Carlo background prediction.

[13] The jet energies used in the mass fitting have been corrected for instrumental and fragmentation effects.